

SUPPORTING INFORMATION

ADEL: Automated Drop-cast Electrode Setup for High-throughput Screening of Battery Materials

Maha Ismail^{1,2}, Maria Angeles Cabañero^{1,4}, Joseba Orive¹, Lakshmipriya Musuvadhi Babulal¹, Javier Garcia¹, Maria C. Morant-Miñana¹, Jean-Luc Dauvergne¹, Francisco Bonilla¹, Iciar Monterrubio¹, Javier Carrasco^{1,3}, Amaia Saracibar², Marine Reynaud^{1*}

1. Centre for Cooperative Research on Alternative Energies (CIC energiGUNE), Basque Research and Technology Alliance (BRTA), Alava Technology Park, Albert Einstein 48, 01510 Vitoria-Gasteiz, Spain.
2. Physical Chemistry Department, Pharmacy Faculty, Basque Country University (UPV/EHU), 01006 Vitoria-Gasteiz, Álava Spain.
3. IKERBASQUE, Basque Foundation for Science, Plaza Euskadi 5, 48009 Bilbao, Spain.
4. FEV Iberia, Calle Cardenal Gardoqui 1, 48008 Bilbao, Spain

* Corresponding author: mreynaud@cicenergigune.com

• S1: ADEL Setup

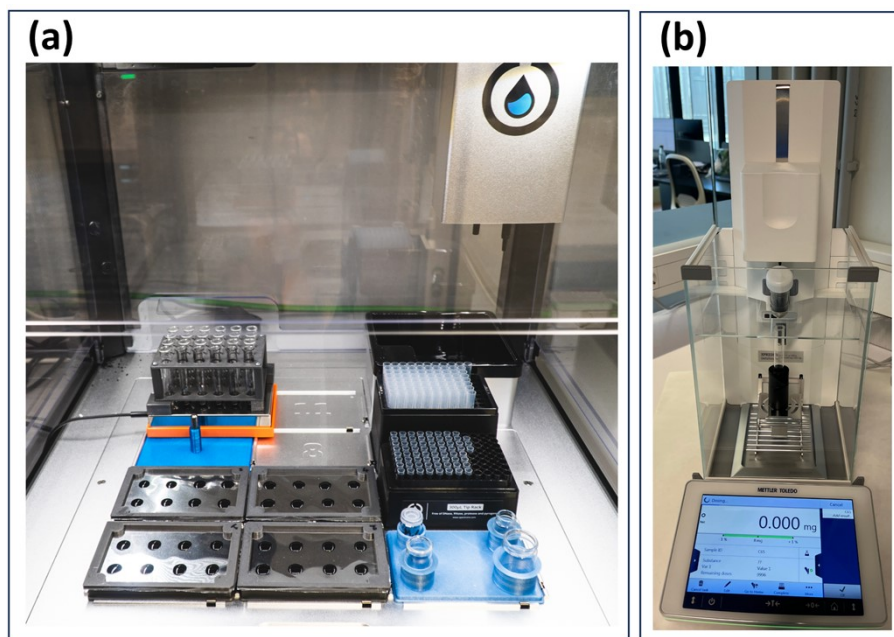


Figure SI- 1: (a) ADEL Setup – photo, (b) automated solid dispenser associated with ADEL setup

A video of the ADEL setup running is provided in the GitHub repository. To run the setup, the protocol designer of the Opentrons robot was sufficient and used to handle all the acts (<https://designer.opentrons.com/>).

Table SI- 1: The aspiration and dispensing parameters used during the pipetting processes offered by the Ot-2 robot supplementary features, such as flow rate of aspiration and dispensing, delay after pipetting, touch tip, and Blowout functions.

	Flow rate of pipetting	Delay after pipetting	Touch tip Option	Blowout Option	Blowout Flow rate
Aspirate	10 $\mu\text{L/s}$	3 sec	On	Off	-
Dispense	19.2 $\mu\text{L/s}$	3 sec	Off	On	270 $\mu\text{L/s}$

- **S2: 3D-printed custom key components:**

- Multi-vial holder design:

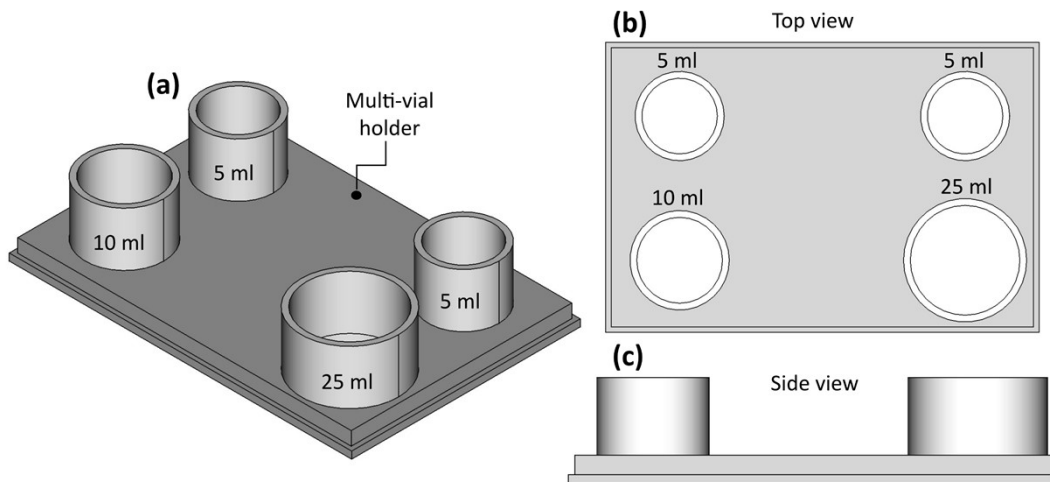


Figure SI- 2: 3D CAD drawings of the multi-vial holder design. a) overview of the multi-vial holder piece showing the 4 wells that can hold up to 4 vials of 5, 10 and 25 mL of liquid. b) top view of the multi-vial holder. c) side view of the multi-vial holder.

- Multi-position Stirring plate holder design:

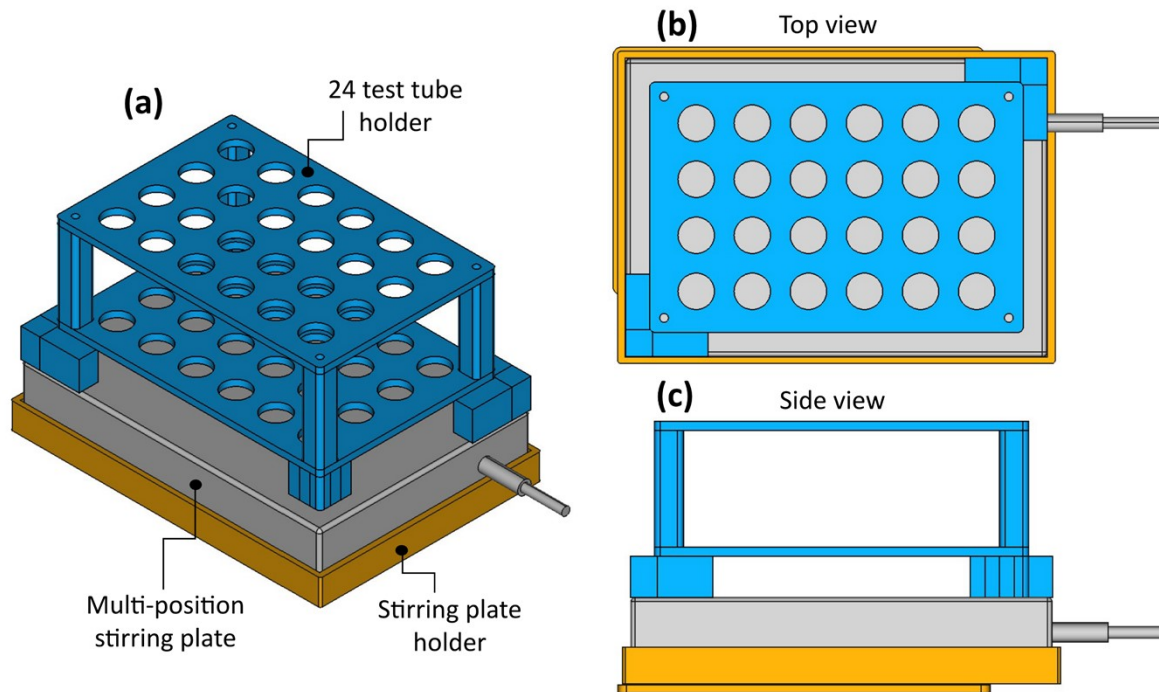


Figure SI- 3: 3D CAD drawings of the multi-position stirring plate holder design: a) overview of the assembly, displaying the multi-position stirring plate and its holder on the Ot-2 desk, with the 24 test tube holder positioned on top. b) top view of the assembly. c) side view of the assembly.

- Al holder design evolution:

The initial design (Figure SI-4-a) used screws to secure the aluminum foil along the edges, but this made it difficult to remove the foil without distorting the electrodes. The second design (Figure SI-4-b) attempted to address the issue by using plastic edges to hold the foil, however, it led to an uneven surface, which distorted the 12 mm electrode shape. In the third design (Figure SI-4-c), the top piece was modified to include eight 12 mm holes for securing the electrode shape, and magnets were added at the corners to fix the Al foil; as a result, the electrode liquid tended to migrate towards the plastic leading to contamination. The final design (Figure SI-4-d) solved these issues by incorporating Neodymium magnets at the holder's corners, ensuring optimal fixation of the Al foil without deforming the electrode shape.

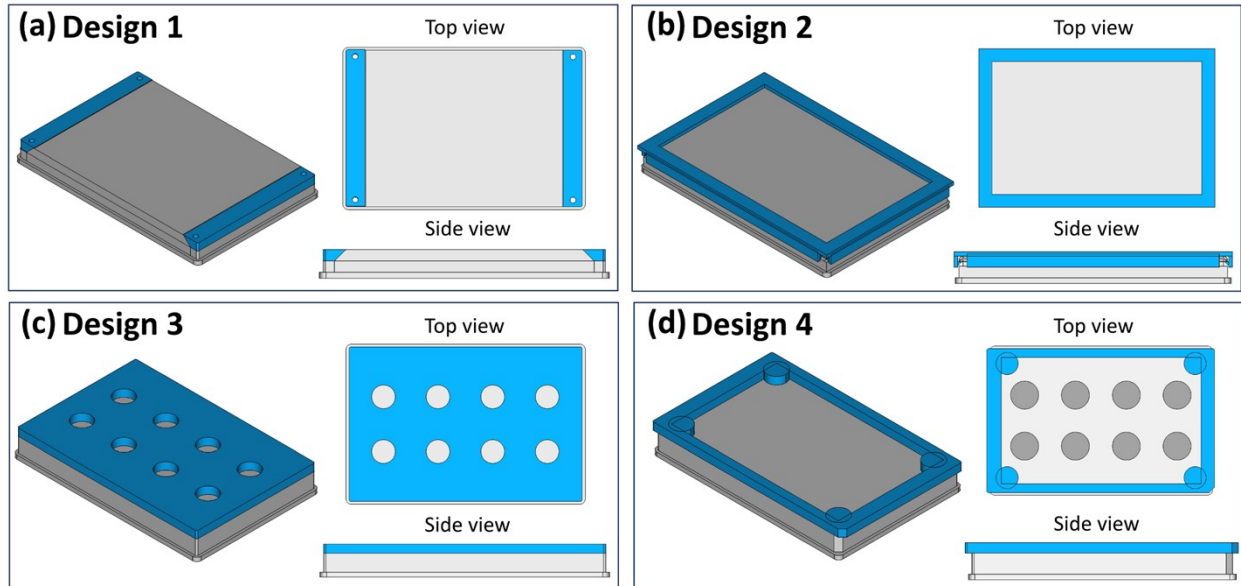


Figure SI- 4: (a-d) 3D CAD drawings of the aluminum foil holder, showing the top and side views of each design from the first to the final version, respectively. The top view of the last version (Design 4) shows that the design was adjusted to ensure that the drop-casted electrodes are well-isolated

The planes of the 2D drawings with the exact measurements of each key component are provided in the GitHub repository.

- **S3: Viscosity tests details:**

The rheological behavior of the Glycerin/water mixtures and the NMC slurry at 23 °C constant temperature, represented in **Figure 2-a**, was measured with a controlled stress rheometer (Haake Series 1 Rheometer) with a plate-plate measuring geometry (PP35Ti, gap 50 mm). The flow curves were measured applying shear rates from 100 - 10000 s⁻¹. The shear rate of the micropipette was calculated employing the Hagen/Poiseuille equation ¹⁻³:

$$\dot{\gamma} = \frac{4 \cdot V}{\pi \cdot R^3}$$

where V is the volume flow rate (V = 10 mm³/s) and R is the radius of the pipette tip (R = 0.21 mm).

- **S4: Drop-casted electrode Drying:**

- Illumination test details:

To assess the homogeneity of the heating system, an aluminum foil (dimension 12.4 x 8.2 cm) was illuminated successively by an infrared lamp (PHILIPS PAR38 IR, 150 W, E27, 230 V Red 1CT/12, see **Figure 3-a**) and a halogen lamp (RS PRO Floodlight, 400 W, interior/exterior, IP44, 220-240 V, see **Figure 3-b**) having a distance of 24 cm between the lamp and the plate in both cases. During both experiments, the thermal behavior of the foil was recorded using an infrared camera (FLIR 325sc). The camera was configured for data acquisition at 2 Hz in a calibrated temperature range of -20 °C to 120 °C. To mitigate background effects and parasitic environmental infrared reflections, the foil was black painted with a high emissivity graphite coating (Kontakt Chemie Graphit 33, CRC Industries Deutschland GmbH). The conversion of the recorded radiometric data into apparent temperatures was carried out using the camera's internal calibration curves and by setting the emissivity to 0.95 (obtained by comparison with data measured with a thermocouple, type T, coupled to a calibrated acquisition system, accuracy +/- 1.0%). Reflected and atmospheric temperatures were considered constant (20 °C). Processing of the recorded data was performed using the FLIR software ResearchIR Max Version 4.40.11.35. The latter consisted in extracting profiles of apparent temperature at different times during the experiments and at different positions near the electrodes (see **Figure 3**).

- Comparison of different drying methods on electrochemical performance:

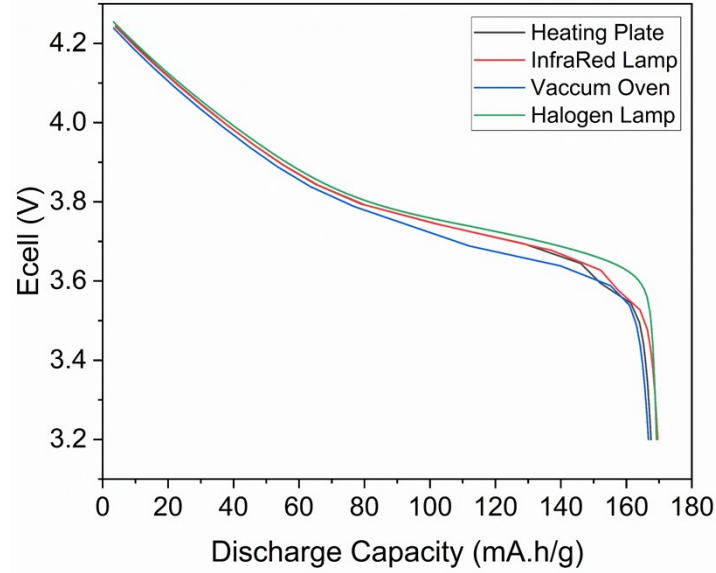


Figure SI- 5: Discharge capacity of NMC-532 cycled at C/20 using different drying methods: vacuum oven, heating plate, infrared lamp, and halogen lamp.

- **S5: NMC-532 Results:**

- Traditional Dr. Blade vs ADEL method:

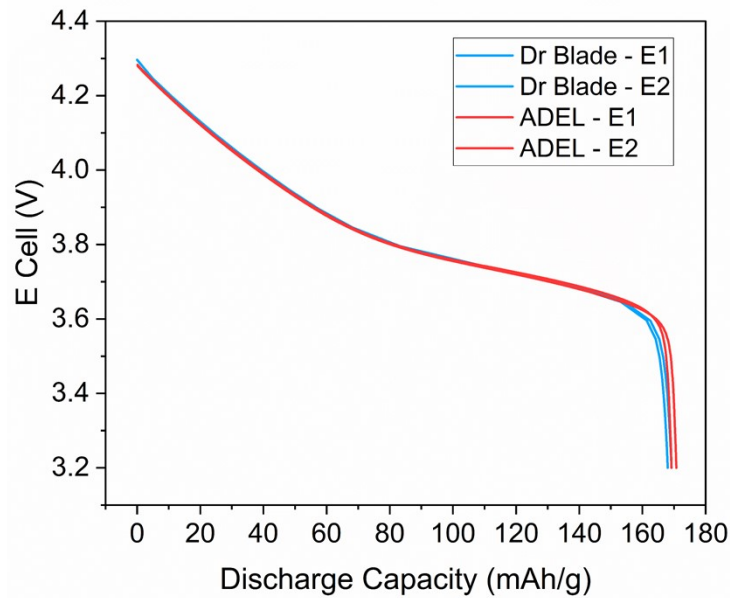


Figure SI- 6: Discharge capacity of 2 electrodes (E1 and E2) of NMC-532 cycled at C/20 prepared by the traditional Dr. Blade method vs ADEL method

- Micro-computed tomography (Micro-CT):

The EasyTom L by RX Solutions is a micro-computed tomography (Micro-CT) system designed for high-resolution, non-destructive 3D imaging, with a spatial resolution of up to 2 μm . It accommodates samples with a maximum diameter of 450 mm, length of 640 mm, and weight of up to 30 kg, making it suitable for a broad range of materials, including ceramics, polymers, and metals. The system is equipped with an open X-ray tube capable of operating at voltages of up to 199 kV and currents of 1000 μA , allowing for optimized scanning conditions tailored to the material under investigation. Image reconstruction and analysis are performed using X-Act (RX Solutions), which enables 16-bit tomographic reconstruction, and VGStudio Max, which facilitates detailed volumetric analysis of internal structures.

In this study, the volumetric reconstruction capabilities of the EasyTom L were utilized to assess the global thickness of an electrode layer deposited on a current collector. An AI-assisted region selection procedure was employed to discriminate between the electrode and the current collector, enabling precise thickness measurements at multiple positions. However, due to the limited field of view (a few square centimeters) of the analyzed areas, the achieved spatial resolution was restricted to the tens of micrometers scale, which did not permit detailed investigation of the electrode's internal microstructure. Consequently, the analysis was confined to global layer thickness measurements rather than nanoscale structural characterization.

To complement the Micro-CT findings, scanning electron microscopy (SEM) analysis was performed on cross-sections of the same samples, prepared using ion milling techniques. This approach enabled high-resolution visualization of microstructural features within individual particles, achieving nanometric spatial resolution. By integrating Micro-CT for macroscopic thickness measurements with SEM for high-resolution microstructural analysis, a multiscale characterization strategy was established, providing a comprehensive assessment of the electrode's structural integrity and material distribution.

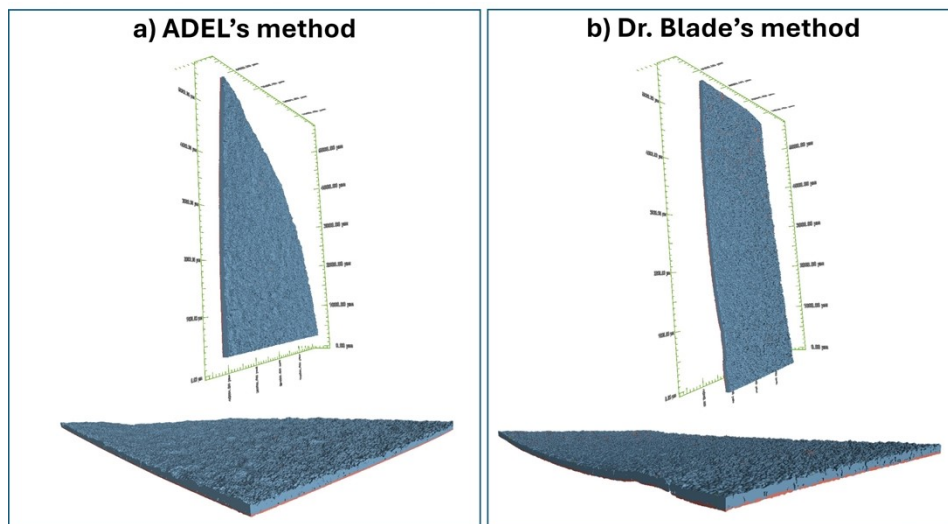


Figure SI- 7: 3D XRCT surface reconstruction of NMC-532 electrodes prepared by (a) ADEL method and (b) the traditional Dr. Blade method.

- IM SEM cross-section details:

The IM4000plus by Hitachi is a versatile ion milling system designed for precise sample preparation in electron microscopy. The system features a high-intensity argon ion source, enabling controlled surface milling and cross-sectioning of materials. Its adjustable voltage range (0.1–6.0 kV) allows for the effective preparation of a wide variety of materials, including metals, ceramics, polymers, and composites. An optimized vacuum chamber ensures controlled milling conditions, minimizing contamination and reducing artifacts during the preparation process.

The IM4000plus has been effectively employed in the preparation of cross-sections of electrode materials, facilitating accurate measurements of layer thicknesses and the identification of critical microstructural features, such as defects, agglomerations, and material segregations. The system's focused ion beam technology produces smooth, undamaged sample surfaces, which are critical for achieving high-resolution imaging and reliable nanometer-scale analysis.

When integrated with scanning electron microscopy (SEM), the IM4000plus enhances the investigation of structural details, material interfaces, and defects. Furthermore, its combination with electrochemical analysis provides a comprehensive understanding of the behavior of electrode materials in battery applications, linking structural and compositional characteristics with performance metrics.

○ NMC-532 data:

Table SI- 2: NMC-532 specific discharge capacity data at different C rates of 2 cycled cells for 2 electrodes prepared from 3 different slurries represented in Figure SI-4

Slurry	Cell	Discharge capacity (mAh/g) at different C rate			
		C/20	C/10	C/50	1C
S1	1	169.71	166.39	160.36	134.01
S1	2	170.09	167.16	161.75	137.35
S2	3	170.74	166.90	160.83	129.73
S2	4	170.63	166.32	160.12	132.95
S3	5	167.56	165.76	160.72	140.59
S3	6	170.06	166.80	161.01	137.21
Average Capacity		169.80	166.56	160.80	135.31
Standard Deviation (SD)		1.06	0.46	0.52	3.51
Relative SD (%)		0.6	0.3	0.3	2.6

Table SI- 3: NMC-532 electrode data including the mass of the active material, the calculated loading, and the specific discharge capacity at different C rates for the represented cells.

Slurry	Cell	mass AM* (mg)	Area (cm ²)	Loading (mg/cm ²)	Discharge capacity (mAh/g) at different C rate							
					C/20	C/20	C/10	C/10	C/5	C/5	1C	1C
1	1	13.877	1.131	12.270	171.65	173.48	169.69	169.80	164.81	164.82	144.63	143.33
1	2	13.079	1.131	11.564	170.6	167.53	168.03	168.74	163.31	163.09	135.07	132.76
2	3	13.748	1.131	12.156	170.84	169.71	168.47	168.7	163.16	162.93	134.02	131.33
2	4	14.094	1.131	12.462	166.47	170.05	168.31	168.13	162.09	161.83	130.12	126.1
3	5	13.705	1.131	12.118	170.22	170.04	169.55	169.91	165.29	165.21	144.77	143.59
3	6	13.776	1.131	12.181	167.69	173.02	169.99	170.14	164.42	164.42	140.3	138.28
4	7	15.018	1.131	13.279	173.17	171.08	170.76	171.53	165.89	165.61	135.89	135.16
4	8	14.825	1.131	13.108	169.19	168.57	167.6	167.77	163.01	162.9	140.92	139.69
5	9	12.449	1.131	11.007	170.71	172.65	169.14	169.15	163.53	163.4	139.05	137.79
5	10	12.464	1.131	11.021	169.09	173.06	169.6	169.79	164.12	164.18	139.47	139.11
Average Capacity		13.70	1.13	12.12	169.96	170.92	169.11	169.37	163.96	163.84	138.42	136.71
Standard Deviation		0.82	0.00	0.72	1.83	1.96	0.94	1.04	1.10	1.14	4.43	5.19
Relative SD (%)		6.0	0.0	6.0	1.1	1.1	0.6	0.6	0.7	0.7	3.2	3.8

*The mass of the active material was calculated using the following methodology: Uncoated aluminum foil, identical to that used in this work, was repeatedly punched into 12 mm discs (7–8 repetitions), and their masses were recorded using a microbalance. The average mass of the foil was determined and used as a baseline, with the active material (AM) mass calculated as 84% of the total mass (reflecting the AM percentage). Monthly checks confirmed the foil's consistent weight, averaging 6.1605 ± 0.0025 mg (minimum: 6.158 mg, maximum: 6.163 mg). This minimal variation in Al foil mass ensured that the foil did not significantly influence observed variations in electrode mass. This methodology was used not only for NMC-532 materials but for all the materials presented within this study.

- **S6: Li-rich materials Results:**

- Li-rich materials data:

Table SI- 4: $\text{Li}_{1.35}(\text{Mn,Ni})\text{O}_2$ discharge capacity data at C/20 and C/10 of the 6 electrodes prepared from 3 different slurries represented in Figure SI-5.

Slurry	Cell	Capacity (mAh/g) at different C rate		
		C/20	C/10	C/10
1	1	275.50	254.28	250.29
1	2	275.40	255.23	251.40
2	3	267.80	243.81	240.41
2	4	271.60	246.41	242.38
3	5	271.60	253.36	251.80
3	6	274.10	255.00	250.95
Average Capacity		272.67	251.35	247.87
Standard Deviation		2.69	4.51	4.64
Relative SD (%)		0.99	1.80	1.87

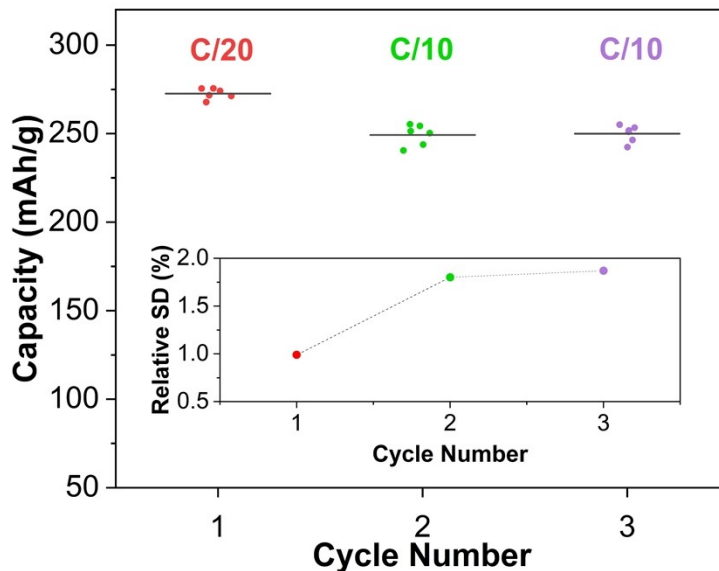


Figure SI- 88: Slurry and electrode reproducibility test showing the specific discharge capacity of the six LMR electrodes (3 slurries; 2 electrodes/slurry) prepared by ADEL module, illustrating the dispersion of the results at C/20 (cycle 1) and C/10 (cycles 2-3). The inset represents the relative % of Standard Deviation of the results at each C rate.

- **S7: Materials Syntheses**

For the synthesis of the $\text{LiFe}_{0.5}\text{Mn}_{1.5}\text{O}_4$ spinel material, a high-throughput sol-gel synthesis approach was used through our automatized synthesis module following the approach reported elsewhere ⁴ with an annealing temperature of 700 °C for 10h.

For the synthesis of Li-rich materials, $\text{Li}_{1+x}(\text{Mn},\text{Ni})\text{O}_2$ cathode materials were synthesized through the solid-state synthesis route. Initially, 1 g of $(\text{Mn},\text{Ni})\text{CO}_3$ precursor (provided by Umicore) was reacted with required amount of Li_2CO_3 through solid-state synthesis route at 60 rpm. The obtained mixture was calcined at 500 °C at 5 h for the precalcination step then it was tuned to anneal at the target temperature (700 to 1000 °C) for 12 h in a muffle furnace via stepping temperature at 5 °C/min.

- **S8: Electrochemical testing**

All the electrodes were prepared with a formulation of 84% of active material, 8% of carbon additive (C65, IMERYS, Switzerland) and 8% of Polyvinylidene fluoride, PVDF binder (Solef 5130/1001, Solvay, Belgium).

NMC-532 electrodes were not calendared, while for LMO, LNMO, LFMO, and LFP, the electrodes were calendared at 2.5 Ton for 30 Sec. Coin cells CR2032 type (MTI) were used for assembling NMC-532 and LFP electrodes, while Swagelok®-type half-cells were used for assembling spinel-type materials (LMO, LNMO and LFMO) and Li-rich materials. All cells were assembled in an Argon-filled glove box using metallic lithium as counter and reference electrodes, and a glass fiber separator soaked in 1M LiPF₆ EC: DMC (Ethylene carbonate: Dimethyl carbonate) electrolyte. Exclusively for the case of LFMO cells, 1M LiPF₆ EC: DMC + 3% FEC (Fluoroethylene carbonate) was used to prevent electrolyte degradation at high voltage. Galvanostatic cycling was performed using Neware model BTS-4000 series battery tester and Biologic VMP3 and BT potentiostats.

The galvanostatic cycling of NMC-532 and LMO cells were performed with the voltage range from 3.2 to 4.3 V versus Li⁺/Li⁰ with a theoretical capacity of 160 mAh/g and 148 mAh/g respectively. The LFP voltage window was from 2.7 to 3.9 V versus Li⁺/Li⁰ with a theoretical capacity of 167 mAh/g. For LNMO, the voltage window was from 3.5 to 3.9 V versus Li⁺/Li⁰ with a theoretical capacity of 147 mAh/g. The LFMO cells were cycled at C/10 with a voltage range from 3.5 to 5.2 V versus Li⁺/Li⁰ and the theoretical capacity was considered to be 148 mAh/g.

• References:

1. Hagen, G. J. A. d. P., Ueber die Bewegung des Wassers in engen cylindrischen Röhren. **1839**, *122* (3), 423-442.
2. Poiseuille, J. L., *Recherches expérimentales sur le mouvement des liquides dans les tubes de très-petits diamètres*. Imprimerie Royale: 1844.
3. Mezger, T., *The rheology handbook: for users of rotational and oscillatory rheometers*. European Coatings: 2020.
4. Monterrubio Santín, I. A high throughput experimental and computational approach for high voltage Mn based spinel materials exploration. Thesis, University of the Basque Country (UPV/EHU), 2023.